Arabian Journal of Chemistry (2021) **14**, 103268

King Saud University

Arabian Journal of Chemistry

www.ksu.edu.sa
www.sciencedirect.com

ORIGINAL ARTICLE

Environmentally friendly catalysts for improved cleaning of toluene-containing gaseous effluents

M. Yates [a], **M.A. Martin-Luengo** [b,*], **A.I. Fernández-Muñoz** [c], **S. Nogales-Velasco** [b]

[a] *Institute of Catalysis and Petrochemistry (ICP, Spanish National Research Council (CSIC)), Spain*
[b] *Institute of Materials Science of Madrid (ICMM, Spanish National Research Council (CSIC)), Spain*
[c] *Centre for hydrographic studies (CEH, Centre for Public Works Studies and Experimentation (CEDEX)), Spain*

Received 23 April 2021; accepted 11 June 2021
Available online 19 June 2021

KEYWORDS

Gaseous effluents cleaning;
Environmentally friendly catalysts;
Eco-friendly process;
toxic particles

Abstract This research describes the design of green oxidation catalysts capable of cleaning toxic gaseous effluents using low cost rice production sub-products, iron oxide chosen as the active phase due to its low toxicity and price (ca. 4 orders of magnitude less than noble metals normally utilised in oxidation reactions) and a low cost abundant clay with excellent rheological properties to facilitate the conformation of the catalysts. These catalysts have activities similar to others which often are based on synthetic and/or expensive and hazardous materials. The use of agro-industrial sub-products lowers the production costs, improves the catalytic performance, leading to a sustainable cycle in which waste materials from an industry are used as renewable raw materials for the same or others. Although addition of palladium (taken as an example of an efficient noble metal for catalytic oxidations) to the best iron containing catalyst, improves the oxidation of toluene decreasing energy costs, there are evidences that its presence in particulates and aerosols produced on use, can cause health problems.

1. Introduction

Global climate change is a serious problem, affecting our lives, and health. Changes are urgently needed to reduce the negative environmental consequences of industrial activities. There seems to be a way to success on changing from activities based on high-carbon energy sources to sustainable more environmentally friendly technologies and consumptions (Yadav et al., 2020) and gaseous effluents are considered as one of the main sources of contamination (Abadi et al., 2020). As part of the scientific community, we believe in using our experience to develop new cleaner compounds and processes, or modifying older more harmful ones, to reduce (or ideally eliminate) those that are dangerous for health and the environment. As an important part of environmental contamination, non-methane volatile organic compounds (NMVOCs) are precursors to ground-level ozone that include a variety of chemicals and processes (solvents, transport, dry-cleaning, raw materials for syntheses, constituent of fuels *etc.*), most are unsafe to human health and produce dangerous photochemical oxi-

---

* Corresponding author.
E-mail address: mluengo@icmm.csic.es (M.A. Martin-Luengo).

Peer review under responsibility of King Saud University.

Production and hosting by Elsevier

https://doi.org/10.1016/j.arabjc.2021.103268
1878-5352 © 2021 The Authors. Published by Elsevier B.V. on behalf of King Saud University.

Nomenclature

RHA	rice husk ash
RB	rice bran
NMVOC	non-methane volatile organic compounds
PGA	pore generating agent
EAC	earth abundant catalysts
EEA	European Environment Agency
TG-DTA	Thermogravimetric-Differential thermal analyser
ICP	Inductively coupled plasma
XRD	X-ray diffraction
MIP	Mercury intrusion porosimetry
GHSV	Gas hour space velocity
FID	Flame ionization detector
IR	Infrared spectroscopy

dants, reacting with nitrogen oxides in the presence of sunlight that must be greatly reduced (EEA).

The present investigation studies the total oxidation with air of toluene, chosen as an example of NMVOC for which noble metals are known to have high catalytic oxidation activities. However, the constituents of environmental catalysts subject to high effluent loads are often released with the exhaust fumes, becoming themselves dangerous, *i.e.* can accumulate in living organisms and pose a threat to both animals and humans (Karimia et al., 2019) and in recent years efforts have been taken towards the development of alternatives, *i.e.* earth abundant catalysts (EAC), amongst them iron, used as active site in this work (Kaushik and Moores, 2017). For these reasons in the present study iron oxide was chosen as the active phase, due to its low toxicity, cost and impact on health and the environment, the amounts of iron chosen to prepare catalysts with activities towards the oxidation of toluene are similar to the ones found in the literature under the reaction conditions used. Furthermore, palladium as example of an element active in this kind of reaction but much more toxic than iron, has been included in the best iron containing catalyst to lower the temperature needed to oxidise toluene.

Moreover, countries with agricultural based economies have vast amounts of crops which generate wastes. Utilising these wastes as low or zero cost renewable raw materials both diminishes contamination and the need for non-renewable materials and if these materials can be employed close to their point of production there are further economic and environmental savings, due to the reduced use of transport and the contamination involved (Gin et al., 2021).

Rice is one of the most important crops worldwide, with an annual world production of ca. 1.2 billion tons. Rice bran (RB) and rice husk (RH) are the major by-products produced in rice milling. Rice bran (RB) is a low cost sub-product, used as raw material in food, cosmetics and pharmaceutical industries, anaerobic digestion, environmental pollution abatement, *etc*. (Schievano et al., 2016). To the best of our knowledge, this is the first time that RB has been used as a pore generating agent (PGA), since we have demonstrated that it favours the interaction between particles acting as an agglomerating agent to form an extrudable paste that is removed on subsequent heat treatment burn out the RB and thus improve the porosity of these conformed ceramic catalysts. Rice husk (RH) has a high silica (ca. 16%) and complex carbohydrate (ca. 82%) contents, it is employed in fertilizers, as a silica source, in environmental remediation, converted to rice husk ash (RHA) in cogeneration plants for use in the steel industry, as adsorbent, catalyst support, construction material, *etc*. (Blissett, et al., 2017; Yates et al., 2011; Suzaimi et al., 2020). In this work RHA from a cogeneration plant is employed to improve textural characteristics in the conformed catalysts improving their catalytic activities, without reducing the compressive strength.

Furthermore, an abundant low cost clay (sepiolite, a magnesium silicate) is employed as the precursor of the structured catalysts, due to its excellent rheological properties that make it an ideal component for extrusion of conformed materials. Another benefit of using this clay is its low aluminium content (ca. 0.5%), given the negative effects of aluminium in the composition of contamination related atmospheric particles that can produce serious diseases, respiration being an important path for the penetration of particles into the human organism (Karimia et al., 2019).

Here catalysts are designed to clean toluene containing gaseous effluents. Given the large volumes of gas that have to be treated, the catalysts need to be structured in order to avoid pressure drop limitations, being this pivotal for their total oxidation efficiency. The catalysts design is based on optimising the microstructural characteristics using agricultural wastes from the rice industry, where rice bran (RB) is introduced as a pore generating agent and rice husk ash (RHA) to improve their compressive strengths, in this way improving the performance of the structured catalysts. Following this development competitive conversions for effluent cleaning to those found in the literature using catalysts that have higher toxicity and are less environmentally friendly, are reached (see *vide infra*).

2. Materials and methods

2.1. Catalysts preparations

The raw materials used in the preparation of the catalysts were iron nitrate nonahydrate ($FeNO_3 \cdot 9H_2O$ 99.5%) and palladium (II) nitrate dihydrate ($Pd(NO_3)_2 \cdot 2H_2O$, 99%) from Panreac, used as precursors of the iron and palladium oxide active phases and low cost residues from rice production (Rice bran (RB) and rice husk ash (RHA). RB used as a Pore Generating Agent (PGA) when it is burnt out of the structured bodies on heat treatment at 500 °C or higher and RHA employed to modify the pore size distribution of the materials to improve their catalytic activities by increasing their total pore volumes and pore widths but avoiding loss in compressive strength. Also sepiolite Pansil (a low cost magnesium silicate from Tolsa S.A.) was employed as the catalyst support due to its ease of extrusion and ability to form ceramic bodies when calcined above 350 °C.

The catalysts were conformed as extrudates to avoid the pressure drop limitations of powder catalysts in high volume effluent gas treatments. The materials were extruded by mixing different amounts of the precursor solids (Sepiolite, RB and RHA) in deionized water with aqueous solutions of the iron and palladium nitrates in an orbital mixer EIRICH model R-02E, with the required volume (ca. 50 wt% water) to attain adequate rheological properties for the subsequent extrusion of the paste with a Bonnot single screw extruder, as solid cylinders with a 3.5 mm external diameter. These extruded materials were allowed to dry at room temperature for 72 h then dried at 150 °C and subsequently heat treated in air at 500 or 700 °C for 4 h, increasing the temperature at 5 °C/min up to the final value in a muffle furnace. These temperatures were chosen from previous experience of working with sepiolite, which undergoes several well documented morphological changes with heat treatment (Yates et al., 2003). The resulting catalysts were denoted as weight compositions of Sepiolite, iron nitrate, RB and RHA (Sep/Fe nitrate/RB/RHA). For comparison purposes the best iron catalyst was impregnated with palladium (II) nitrate dihydrate and further calcined at 500 °C to decompose the precursor salt.

2.2. Catalysts characterisation

The thermal behaviours of both the raw materials and the conformed composites were analysed to study their stabilities in a TG-DTA Stanton model STA 781, heating them from room temperature to 900 °C at a heating rate of 10 °C/min, in an air flow of 20 ml/min. Based on these TG-DTA analyses, each precursor dough was treated at three temperatures: 150, 500 and 700 °C, to dry, decompose and modify the activities porosities, surface areas and compressive strengths of the final materials.

The elemental analyses of the solids were carried out employing inductively coupled plasma (ICP) in a Perkin-Elmer, model Optima 3300 DV. The crystalline characteristics of the materials were analysed by X-ray diffraction in a Seifert model XRD 3000P in the range $2\theta = 5–75°$, with a 0.02°/step and acquisition time of 2 sec/step.

Transmission electron microscopy was carried out in a JEOL model FXII electron microscope operating at 200 kV, on solids deposited on carbon covered copper grids.

The textural characteristics of the materials were determined using nitrogen adsorption at 77 K and mercury intrusion porosimetry. The ads-desorption isotherms were carried out in a Micromeritics ASAP 2020 apparatus, on samples that had been previously outgassed to a vacuum of 10^{-2} Pa during 16 h, to ensure clean dry surfaces that were free from any loosely bound adsorbed species. For the materials dried at 150 °C the outgassing procedure was carried out at this temperature. The materials heated to 500 °C or higher were outgassed at 300 °C. The volumes and pore size distributions of pores with diameters higher than 7.5 nm were determined by mercury intrusion porosimetry (MIP) on a Fisons Instruments Pascal 140/240 apparatus, using *ca.* 0.2 g of material that had been previously dried at 150 °C for 16 h. The pressure/intrusion data were analysed by the Washburn equation, taking the recommended values for the mercury contact angle (141°) and surface tension (484 mN/m).

The compressive strengths of the composites were measured on a dynamometer Chatillon model LTMC, by means of applying a pressure on the external surface of the extrudates until breakage, with a test head of 1.32 cm^2. The rupture pressure ($kg\ cm^{-1}$) was taken as the average value of 10 measurements.

Basicity analyses were performed to study the amount and strength of the basic centres on the composites by the desorption/decomposition of acetic acid previously adsorbed onto the materials, using a TG/DTA Stanton 781 coupled to a mass spectrometer Thermostar QMS200 M3 and analysing both the amount and temperature at which CO_2 was produced by the decomposition of the acetic acid on increasing the temperature from room temperature up to 900 °C at 10 °C min^{-1}.

2.3. Toluene oxidation

The catalytic activity for the total oxidation of toluene was carried out in a stainless steel fixed bed reactor (internal diameter 3.5 cm length 85 cm), with silica wool in the inside at half height and a quartz tube of 12 mm internal diameter and 14 mm external diameter. The free space between the quartz tube and the reactor wall was filled with silicon carbide of particle sizes lower than 0.84 mm, to fix the quartz tube in place. The temperature was controlled by means of two thermocouples at different heights inside the reactor. The catalytic activity was measured using the cylindrical extrudes of 1 cm in length. Approximately 50 ml/min air flow was bubbled through toluene maintained at −12 °C in a cryostat, that was then diluted with more air in order to attain a total air flow of 3500 ml/min with 100 ppm of toluene, at a constant gas hour space velocity (GHSV) of 35000 h^{-1} and a linear velocity of 0.52 m/s for all experiments. The toluene concentrations at the inlet and outlet of the reactor were analysed with a Flame ionization detector (FID, Horiba FIA – 510) and the CO_2 produced on total oxidation was measured in a Horiba VIA-510 Analyser by infrared spectroscopy (IR).

3. Results and discussion

3.1. Characterisation of precursors and catalysts

The catalysts nomenclature is based in amounts by weight of Sep/Fe/RB/RHA, the palladium containing catalyst is denoted as Pd 17/2/2/2. TG-DTA analyses of the calcination of the precursors indicated that the decomposition of rice bran (RB) (Fig. 1a) gave rise to two exotherms at 250 °C and 430 °C due to the combustion of carbohydrates (Martin-Luengo et al., 2011), with a total weight loss close to 90%. Chemical analyses of the remnant material indicated it was silica. The thermal analysis on rice husk ash (RHA) (not shown) did not lead to any significant weight loss, as expected, since it had been prepared by incinerating rice husk waste from rice production at 850 °C in the factoryś cogeneration plant.

Iron nitrate nonahydrate decomposes below 200 °C, with an endotherm at 80 °C due to loss of physisorbed water, another at *ca.* 115 °C due to the loss of seven molecules of water of hydration, with the rest of the water molecules and decomposition of nitrates occurring at 195 °C, with a total weight loss of *ca.* 73% (Fig. 1b).

The thermal behaviours of extruded Fe/Sep (17/1/0/0, Fig. 1c) and sepiolite (17/0/0/0 Fig. 1d) were similar, with an endotherm at 130 °C due to loss of adsorbed water, another

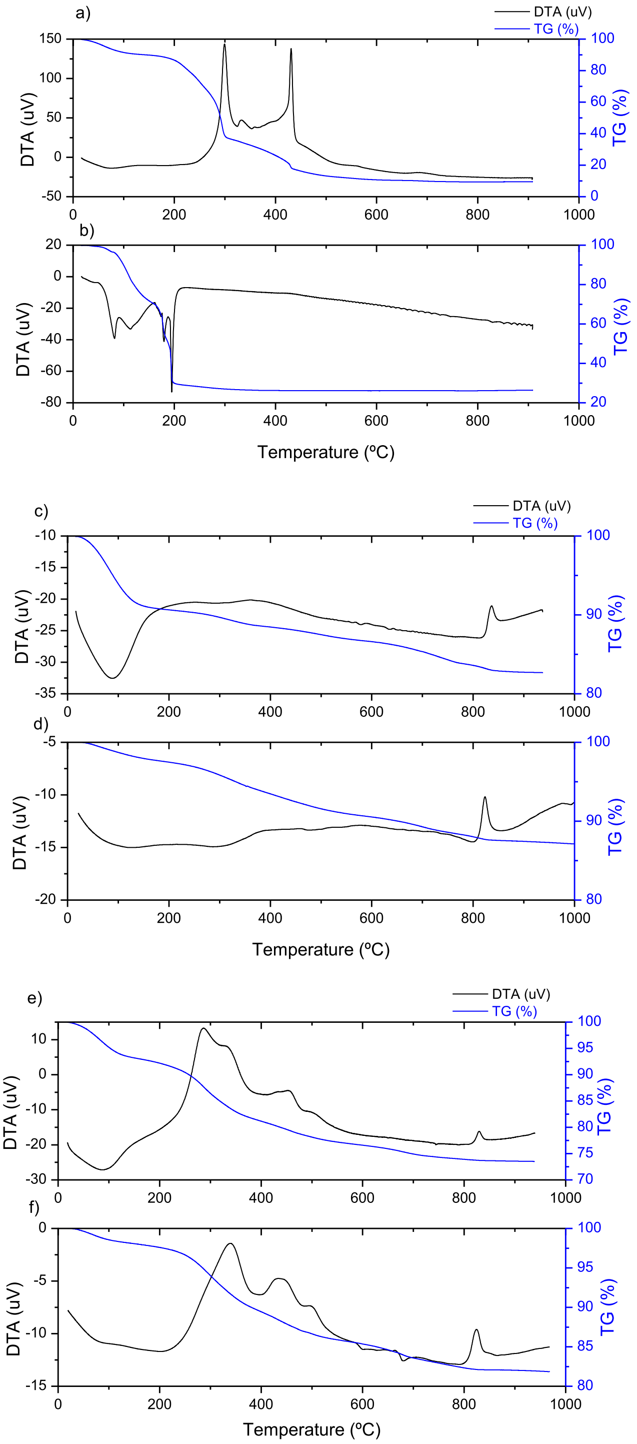

Fig. 1 TG-DTA thermograms of catalyst precursors (Sep/FE/RB/RHA): a) 0/0/RB/0b) Fe(NO_3)$_2$ 6H_2Oc) 17/1/0/0d) 17/0/0/0e) 17/2/2/2f) 17/1/2/2.

at 290 °C due to loss of zeolitic water that occupies the sepiolite channels, at 475 °C loss of crystallization water attached to silicon and magnesium terminal ions of the octahedral layer of sepiolite, causing a collapse of its internal structure, another endothermic peak at T > 500 °C due to loss of constitutional water, which forms part of the structure as hydroxyls, and an exotherm at about 827 °C due to phase transformation of sepiolite to enstatite (Yates et al., 2003). From previous results it is known that treatment of the extrudates at 500 °C leads to the transformation of sepiolite into a stable ceramic material that cannot be rehydrated due to the loss of constitutional water and the folding of the structure at a temperature of approximately 330 °C. With heat treatment at 700 °C the structure gains compressive strength but suffers a reduction in the surface area due to sintering of the material.

The thermograms of the catalysts precursors were a mixture of the decomposition of the various components, as expected, materials 17/2/2/2 (e) and 17/1/2/2 (f), are chosen as examples. According to the TG-DTA results a minimum temperature of 500 °C in air was enough to decompose the various precursors and produce the conformed ceramic catalyst and 700 °C was also chosen in order to check the effect of a higher calcination temperature on the catalytic activities. Although heat-treatment at higher temperatures increases the compressive strengths, this is achieved at the expense of a notable reduction in the specific surface area of the material.

The compositions of the catalysts precursors and percent composition of the catalysts after calcination were analysed by Inductively Coupled Plasma (ICP) (Table 1). Due to its natural origin, sepiolite contains 28% silicon, 12% magnesium, 2.5% calcium, 0.9% potassium, 0.7% iron, 0.7% phosphorous and less than 0.5% for aluminium and sodium. The content of alkaline and alkaline earth cations and iron gives sepiolite its basic character.

X-ray diffraction analysis of the crystallinities of precursors and catalyst 17/2/2/2 treated at different temperatures, chosen as examples are shown in Fig. 2. As expected, catalyst 17/2/2/2 treated at 150 °C gave rise to the characteristic peak for sepiolite at $2\theta = 7.2°$, related to the microporous channels, which on heating above 350 °C disappeared due to the collapse and folding of the structure. The characteristic main reflexion peaks for iron oxides were not present in the XRD patterns, being for Fe_2O_3 at 35.7° (JCPDS No. 39–1346) and Fe_3O_4 at 34.8° (JCPDS No. 75–0033). Furthermore, the XRD patterns of catalysts 17/2/2/2 and Pd 17/2/2/2 are identical and no PdO oxide is detected at 33.8° (JCPDS No. 41–1107). The results support the good dispersions achieved with this production technique, since crystals with sizes of less than *ca.* 4–5 nm cannot be detected by XRD. The peaks at 26.5° and 22° were due to quartz and cristobalite present in the sepiolite.

Analyses of textural properties by nitrogen adsorption–desorption and mercury intrusion porosimetry indicated (Table 1 and Fig. 3) that as the heat treatment temperature was increased there was a reduction in the overall pore volume (V_t) and higher temperatures caused an increase of compressive strengths (see Table 1). When iron was added (17/1/0/0) the overall pore size distributions observed were similar to those of sepiolite (17/0/0/0) extrudates although slightly shifted to wider pores and giving rise to an increase in the total pore volume. For the material that incorporated both iron and RB (17/1/2/0) there was a substantial increase in both the overall pore volume and pore widths, with the formation of a more open porous structure in this incorporated catalyst, that would lead to a reduction in any diffusion limitations and positively affect the catalytic activity (Mazaheri et al., 2018). As shown in Table 1, the palladium containing catalyst (Pd 17/2/2/2) did not show differences in its textural characteristics versus its non-palladium containing counterpart (17/2/2/2).

The catalyst that contained sepiolite, iron and RHA (17/1/0/2) gave rise to a distinct bimodal cumulative pore vol-

Table 1 Compositional, structural and textural characterization of catalysts.

Sep/Fe/RB/RHA**	%Pd	%Fe	S_{BET}^{a}	V_t ^b	V_{mes}^{c}	V_{mac} ^d	d_p^e	MS^f
17/0/0/0	–	0.7	136	0.54	0.42	0.12	52	226
17/1/0/0	–	2.2	143	0.56	0.42	0.14	56	181
17/1/0/0*	–	2.2	110	0.47	0.32	0.15	61	230
17/1/2/0	–	2.2	140	0.72	0.41	0.31	200	165
17/1/0/2	–	2.3	125	0.66	0.33	0.33	201	186
17/1/2/2	–	2.0	144	0.79	0.35	0.44	81	158
17/1/2/2*	–	2.0	91	0.63	0.16	0.47	91	257
17/1/2/2 (x3)	–	2.0	142	0.78	0.36	0.42	81	164
17/2/2/2	–	3.1	104	0.72	0.32	0.39	72	135
Pd 17/2/2/2	1.6	3.1	106	0.70	0.31	0.43	71	136

Calcined at 500 °C (except * at 700 °C).
a: Surface Area (m^2g^{-1}).
b: Total Pore Volume (cm^3g^{-1}).
c: Mesopore Volume (mes).
d: Macropore Volume (mac).
e: d_p Pore diameter (nm).
f: Compressive Strength ($Kg.cm^{-1}$).
**Other elements due to sepiolite composition are 28% silicon, 12% magnesium, 2.5% calcium, 0.9% potassium, 0.7% iron, 0.7% phosphorous and less than 0.5% for aluminium and sodium.
Standard deviations in ICP analyses are typically less than 0.1%.

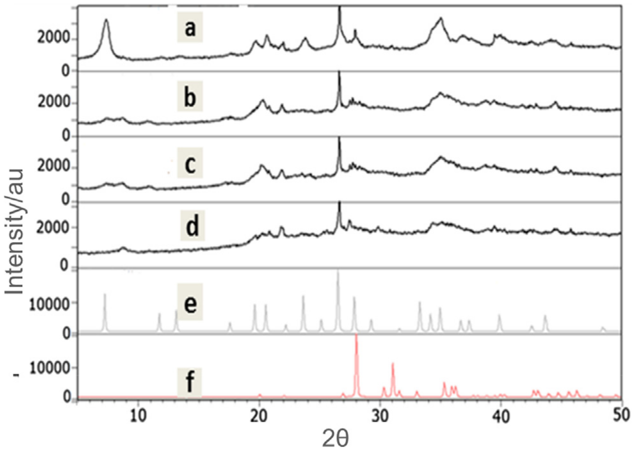

Fig. 2 XRD patterns of Sep/Fe/RB/RHA (17/2/2/2) (a) 150 °C, (b) 500 °C, (c) 700 °C, (d) 850 °C, (e) sepiolite (17/0/0/0), (f) enstatite.

ume curve with the usual porosity in pores below about 200 nm due to the sepiolite but an additional porosity in pores close to 1 µm due to the interparticulate porosity between the primary particles of the RHA. The presence of these much wider pores greatly reduces any diffusional limitations of these incorporated catalysts, thus leading to a marked increase in the catalytic activity. The catalysts prepared by calcining at 500 °C, had porosities that benefitted from the advantages of both using the PGA and the RHA: increased overall pore volumes and the presence of much wider macropores, close to 1 µm (Fig. 3).

The effect of the compositions and heat treatments of the structured catalysts on their compressive strengths are shown in Table 1. From these results it was clear that the catalysts with higher compressive strengths were those treated at 700 °C and the weakest those treated at 500 °C. This was to be expected since initial heat treatment at 500 °C causes the degradation of any PGA and a significant increase in the total pore volume of the composite, whilst heat treatments at higher temperatures then leads to sintering of the ceramic material and phase changes which reduces the total pore volumes and improves the compressive strengths (Yates et al., 2003).

Regarding the dimensional stability of the materials, as the heat treatment temperature was increased the exterior dimensions of the conformed materials were reduced due to the corresponding increase in their densities. From these results, high heat treatment temperatures would be the best choice to achieve better compressive strengths and abrasion resistances, but this must be balanced with the loss in specific surface area and consequent loss in catalytic activity.

Analyses of basic oxidation sites were carried out using TG-MS, monitoring the desorption/decomposition of acetic acid previously adsorbed onto the catalysts surfaces forming carbonate, bidentate or bridged acetate species. By recording the intensities and positions of the peaks corresponding to the decomposition of these entities to CO_2 (m/e 44) both the amount and strength of basic sites, closely related to their catalytic oxidation activities were determined. The areas and intensities indicate the amounts of basic centres and their strengths are related to the temperatures at which the bands are observed (Fig. 4) (Yates et al., 2017a).

From previous studies it has been shown that the desorption/decomposition of acetic acid at temperatures below 250 °C were related to the amount of low strength basic sites, while those at 350–550 °C were due to medium and high strength basic centres: Mg-O (and Mg-O-H) and Fe-O (and Fe-O-H) (Yates et al., 2017). Fig. 4 indicates that sepiolite has small amounts of basic centres of low, medium and high strengths, as expected due to its content of alkaline and alkaline earth cations (12% magnesium, 2.5% calcium, 0.9% potassium) and 0.7% iron and it can also be seen that for the catalysts calcined at 500 °C, 17/1/0/0 has similar amount of basic sites to its counterparts that contain RB and RHA (17/1/2/0, 17/1/0/2 and 17/1/2/2). The catalyst with a

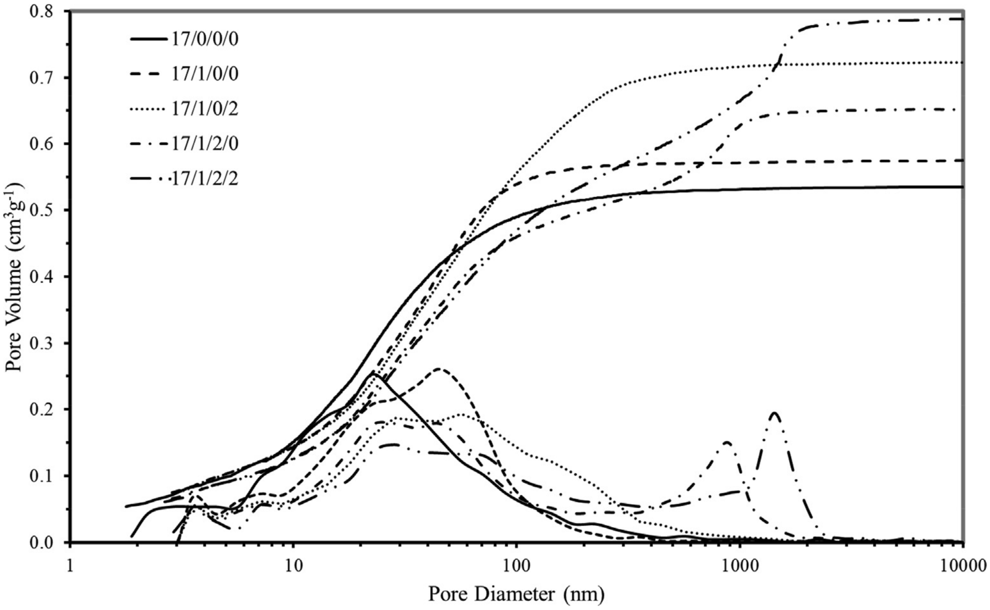

Fig. 3 MIP of catalysts (Sep/Fe/RB/RHA) calcined at 500 °C.

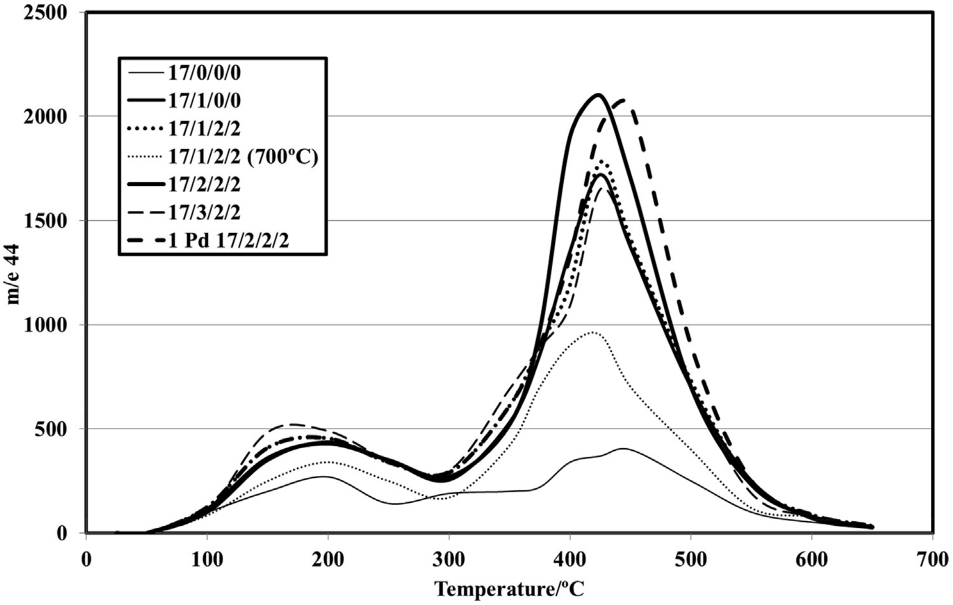

Fig. 4 Basicity analysis of catalysts after acetic acid adsorption (m/e 44 *vs* Temperature).

higher amount of iron (17/2/2/2) has larger amounts of strong basic centres and catalyst 17/1/2/2 showed lower amount of strong basic sites than 17/2/2/2 due to sintering of the active phase. It should also be noted that on increasing the calcination temperature the amount of high strength basic sites decreases, in agreement with the loss in surface area. The palladium containing catalyst (Pd 17/2/2/2) shows similar amount of basic sites as catalyst 17/2/2/2, but it has a greater amount of high strength basic sites (peak at ca 439 °C) due to the displacement of the temperature of strong basic sites to higher values (see Fig. 4).

Transmission electron micrographs of the catalysts were used to recover information on the morphology and particle size of iron oxide catalysts (Fig. 5) showing lower dispersion of the iron phase in the catalyst with higher amount of iron, in agreement with the lower amounts of basic sites found, due to sintering of the iron oxide species and with the lower activities found for the catalyst with higher amount of iron added. The importance of this parameter is related to the oxidation activities (see below).

3.2. Toluene oxidation

The catalytic activity tests showed no reaction products other than H_2O and CO_2 under the conditions used in this work. Repeated catalytic runs were reproducible for at least three consecutive reactions, without any appreciable loss in activity, indicating the robustness of the conformed catalysts.

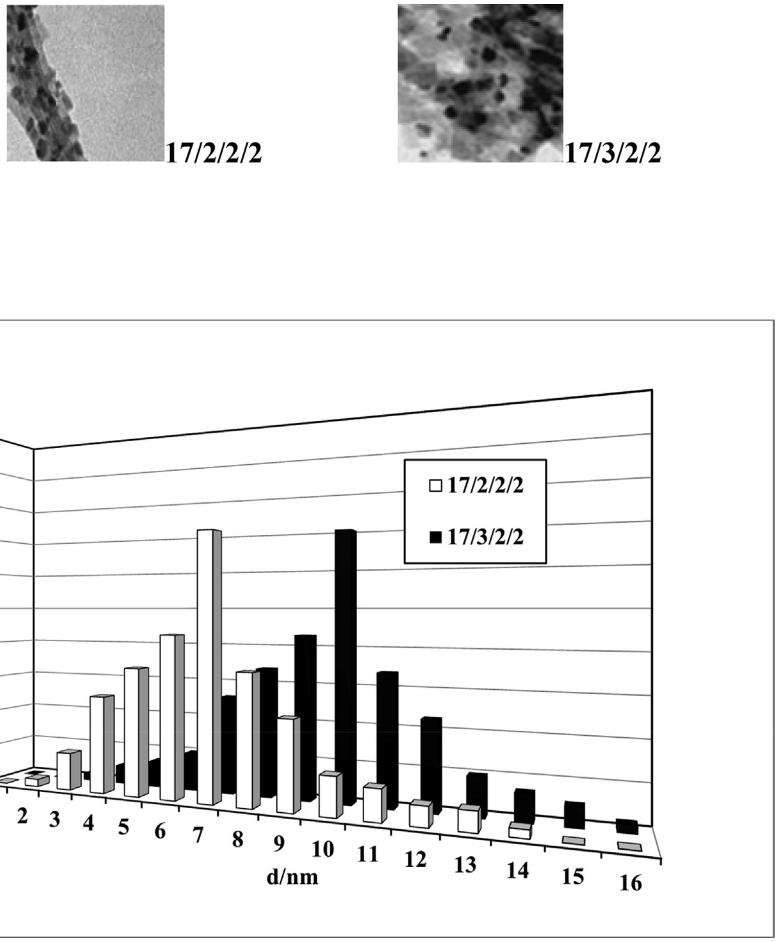

Fig. 5 Transmission electron micrographs and particle size distributions of catalysts.

In this work the amounts of strong basic sites measured by acetic acid adsorption–desorption/decomposition (Fig. 4) are related to the order of activities (see Fig. 6 and Table 2), being related to loss of active surface area by agglomeration of the iron oxide particles, by increasing the temperature of calcination or the amount of iron with the consequent loss of activity (Aguayo-Villareal, 2017; Nogueira et al., 2011).

Moreover, in agreement with the proposed mechanism, the addition of RB and/or RHA result in improved catalytic activities where the textural analyses indicate that there are increases in both pore width and pore volume of the catalysts on adding these components, *i.e.* the presence of RHA in the catalysts produces pores of *ca*. 900 nm, and on adding RB the pore volumes are increased and therefore the molecules of toluene will reach more easily the active phase (Szegedi et al., 2013). In agreement with these, the activities for the catalysts calcined at 500 °C were higher than those of their counterparts calcined at 700 °C (Yates et al., 2017), since, although an increase in calcination temperature improves the compressive strength, the decrease in surface area and pore volume on calcining at 700 °C with the consequent loss of the active basic sites causes a reduction in their catalytic activities.

From the characterisation and activity results, the best catalytic activity for total oxidation of toluene of the iron containing catalysts is due to the favourable combination of the surface properties, and the better dispersion of the active oxide phases (Boycheva et al., 2019; Nogueira et al., 2011).

Judicious choice of components and thermal treatments allow us to achieve catalysts that have activities similar to those found for similar processes in published work, although often those are based on synthetic and/or expensive materials, or using potentially dangerous compounds and are therefore less environmentally acceptable than the green catalysts developed in this work (Markova-Velichkova et al., 2013).

Addition of palladium to the best iron containing catalyst, improves the oxidation of toluene with values similar to other published palladium containing catalysts (Kima et al., 2015) (Table 2 and Fig. 6), due to its content of higher amounts of strong basic sites compared to its non-palladium containing counterpart (17/2/2/2). However, palladium and its compounds are known to be highly toxic, especially compared to those of iron (Kaushik and Moores, 2017; Egorova et al., 2019) and therefore its presence in particulates that are produced during use has to be taken into account. Lower energy and therefore costs have to be considered versus the problems caused by toxics contained in the catalysts which are released into the atmosphere due to abrasion during use.

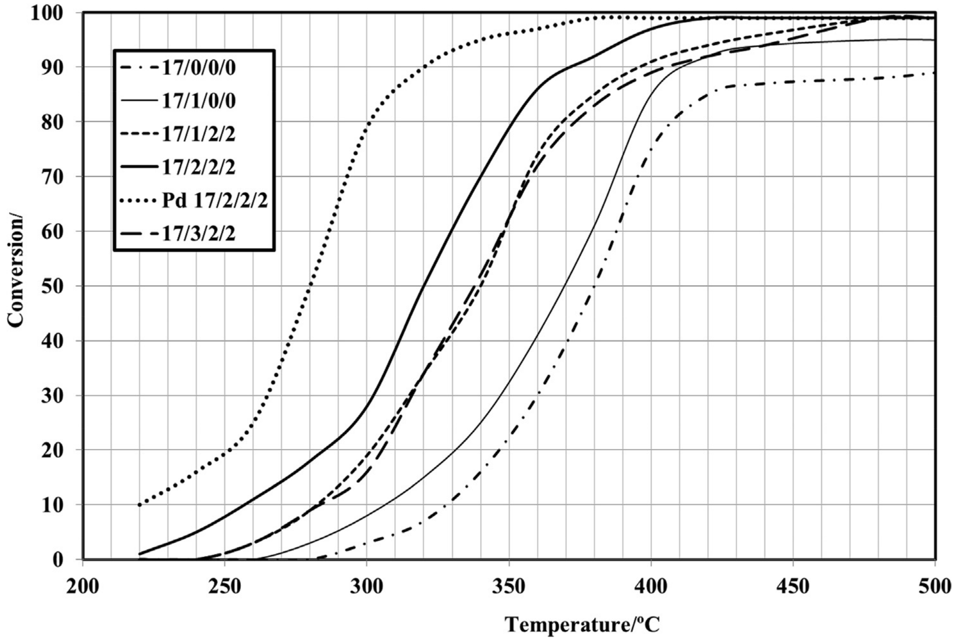

Fig. 6 Catalytic oxidation of toluene (Conversion (%) *vs* Temperature (°C)).

Table 2 Catalytic oxidation of toluene on catalysts calcined at 500 °C (Temperatures of 10%, 50% and 90% conversion (°C) are included).

Sep/Fe/RBA/RHA	T_{10}	T_{50}	T_{90}
17/0/0/0	351	430	502
17/1/0/0	304	360	443
17/1/0/0*	313	388	471
17/1/2/0	305	352	425
17/1/0/2	279	344	412
17/1/2/2	275	346	407
17/1/2/2*	304	370	451
17/1/2/2 (x3)	275	354	427
17/2/2/2	261	334	407
17/3/2/2	278	340	409
Pd 17/2/2/2	220	280	320

4. Conclusions

Catalysts conformed with innocuous components (rice production residues, iron and a local clay) were designed to decontaminate toluene containing gaseous effluents, thus avoiding expelling toxic compounds in catalyst treated exhausts gases to the atmosphere during use.

The design of adequate microstructure, texture and composition of the catalysts allows the presence of accessible basic sites that make them active in the oxidation of toluene, chosen as an example of NMVOC where conversions were reached that are competitive with results found in the literature which often use toxic and expensive components. The catalysts calcined at lower temperatures had higher amounts of strong basic sites and consequently higher activities. These were also more economic and environmentally friendly compared to those currently used today due to their compositions and sustainable origin. Furthermore, conformation of the catalysts avoids pressure drop, allowing them to be used in industrially relevant conditions for gaseous effluent decontamination.

It must be stressed that although addition of palladium to the best iron catalyst increases the amount of high strength basic sites and therefore improves the catalytic oxidation of toluene, the hazards produced by palladium related toxic compounds should be taken into consideration.

Declaration of Competing Interest

The authors declare that they have no known competing financial interests or personal relationships that could have appeared to influence the work reported in this paper.

Acknowledgements

The authors wish to acknowledge the financial support of the Spanish National Research Council (CSIC) for the projects “Preparation of materials from agro industrial residues” (PIE CSIC 201480E103) and “Valorisation of Spanish agriresidues for advanced uses” (PIE CSIC 201460E105) and the Centre for the Development of Industrial Technology (CDTI) for projects “Systems to recycle aqueous effluents with valorisation. Total oxidation of contaminants” (IDI-20091139), “Development of applications of sub-product of biodiesel with own company′s catalysts made from Ecomaterials” (IDI-20121298). “Design of silica of controlled texture to use in detergents from rice residues” (IDI-201443711). “Exploitation of agroindustrial residues for advanced uses. Climate change, Sustainable development and Circular Economy” (IDI-202180E025).

References

Abadi, M.B.H., Shirkhanloo, H., Rakhtshah, J., 2020. Air pollution control: The evaluation of TerphApm@MWCNTs as a novel heterogeneous sorbent for benzene removal from air by solid phase gas extraction. Arab. J. Chem. 13, 1741–1751.

Aguayo-Villarreal, I.A., 2017. Importance of iron oxides on the carbons surface vs the specific surface for VOC's adsorption. Ecol. Eng., 106, Part A, 400-408.

Blissett, R., Sommerville, R., Rowson, N., Jones, J., Laughlin, B., 2017. Valorisation of rice husks using a TORBED® combustion process. Fuel Proc. Technol. 159, 247–255.

Boycheva, S., Zgureva, D., Václavíková, M., Kalvachev, Y., Popova, M., 2019. Studies on non-modified and copper-modified coal ash zeolites as heterogeneous catalysts for VOCs oxidation. J. Hazard. Mater. 361, 374–382.

Egorova, Ksenia S., Sinjushin, Andrey A., Posvyatenko, Alexandra V., Eremin, Dmitry B., Kashin, Alexey S., Galushko, Alexey S., Ananikov, Valentine P., 2019. Evaluation of phytotoxicity and cytotoxicity of industrial catalyst components. Fe, Cu, Ni, Rh and Pd. Chemosphere 223, 738–747.

European environment Agency (EEA, Air-pollution-country-fact-sheets, http://WWW.eea.europa.eu).

Gin, A.W., Hassan, H., Ahmad, M.A., Hameed, B.H., Mohd Din, A.T., 2021. Recent progress on catalytic co-pyrolysis of plastic waste and lignocellulosic biomass to liquid fuel: The influence of technical and reaction kinetic parameters. Review. Arab. J. Chem. 14. 103035.

Karimia, B., Shokrinezhada, B., Samadib, S., 2019. Mortality and hospitalizations due to cardiovascular and respiratory diseases associated with air pollution in Iran: A systematic review and metaanalysis. Review article. Atmos. Env. 198, 438–447.

Kaushik, M., Moores, A., 2017. New trends in sustainable nanocatalysis: Emerging use of earth abundant metals. Curr. Opin. Green Sust. Chem. 7, 39–45.

Kima, S.C., Nahma, S.W., Parkba, Y.K., 2015. Property and performance of red mud-based catalysts for the complete oxidation of volatile organic compounds. J. Hazard. Mater. 300, 104–113.

Markova-Velichkova, M., Lazarova, T., Tumbalev, V., Ivanov, G., Naydenov, A., 2013. Complete oxidation of hydrocarbons on YFeO3 and LaFeO3 catalysts. Chem. Eng. J. 231, 236–245.

Martin-Luengo, M.A., Yates, M., Diaz, M., 2011. Renewable fine chemicals from rice and citric subproducts. Ecomaterials. ppl. Catal. B Env. 106, 488–493.

Mazaheri, H., Ong, H.C., Masjuki, H.H., Amini, Z., Alwi, A., 2018. Rice bran oil based biodiesel production using calcium oxide catalyst derived from Chicoreus brunneus shell. Energy 144, 10–19.

Nogueira, F.G.E., Lopes, J.H., Silva, A.C., Lago, R.M., Fabris, J.D., Oliveira, L.C.A., 2011. Catalysts based on clay and iron oxide for oxidation of toluene. Appl. Clay Sci. 51, 385–389.

Schievano, A., Sciarria, T.P., Gao, Y.C., Scaglia, B., Adani, F., 2016. An integrated system to valorize swine manure and rice bran. Waste Manag. 56, 519–529.

Suzaimi, N.D., Goh, P.S., Malek, N.A.N.N., Lim, J.W., Ismail, A.F., 2020. Enhancing the performance of porous rice husk silica through branched polyethyleneimine grafting for phosphate adsorption. Arab. J. Chem. 13, 6682–6695.

Szegedi, A., Popova, M., Lázár, K., Klébert, S., Drotár, E., 2013. Impact of silica structure of copper and iron-containing SBA-15 and SBA-16 materials on toluene oxidation. Microp. Mesop. Mater. 177, 97–106.

Yadav, R., Baskaran, T., Kaiprathu, A., Ahmed, M., Bhosale, S.V., Joseph, S., Al-Muhtaseb, A.H., Singh, G., Sakthivel, A., Vinu, A., 2020. Recent advances in the preparation and applications of organofunctionalized porous materials. Chem.-An Asian J. 15, 2588–2621.

Yates, M., Blanco, J., Martín-Luengo, M.A., Martín, M.P., 2003. Vapour adsorption capacity of controlled porosity honeycomb monoliths. Microp. Mesop. Mater. 65, 219–225.

Yates, M., Díaz, M., Martin-Luengo, M.A., 2011. Renewable fine chemicals from rice and citric subproducts: Ecomaterials. Appl. Catal. B: Env. 106, 488–493.

Yates, M., Huerta, D., Martin-Luengo, M.A., 2017. Three pathways to cleaner platform chemicals: Conventional, microwave and solar transformation of a by-product from the orange juice manufacturing process. J. Clean. Prod. 168, 746–754.